Geometric Design of Fluid Segments in Microreactors Using Dimensionless Numbers

Nobuaki Aoki, Shinji Hasebe, and Kazuhiro Mae
Dept. of Chemical Engineering, Graduate School of Engineering, Kyoto University, Kyoto-daigaku Katsura, Nishikyo-ku, Kyoto 615-8510, Japan

DOI 10.1002/aic.10727
Published online November 14, 2005 in Wiley InterScience (www.interscience.wiley.com).

In microreactors, reactant fluids are split into many fluid segments and then fed into the reactors to shorten mixing time. Two dimensionless numbers are introduced to represent effects of geometric design factors of fluid segments, such as shapes and arrangements, on reactor performance, namely mixing rate and product yield and selectivity: the ratio of reaction rate to diffusion rate and the aspect ratio of the mean diffusion length in the two-dimensional (2-D) directions in the reactor cross section. Methods to determine these numbers are also proposed. To examine the validity of these numbers on estimating the reactor performance, we compare product yields between each pair of reactors having the different geometric design factors but the same dimensionless numbers using computational fluid dynamics simulations. The results show that these numbers serve as the indices for estimating the reactor performance. Using these numbers, design guidelines for geometry of fluid segments are also discussed. © 2005 American Institute of Chemical Engineers *AIChE J,* 52: 1502-1515, 2006

Key words: microreactor, geometry of fluid segments, dimensionless number, molecular diffusion, product yield and selectivity

Introduction

Microreactors have received significant research interest and have been identified their potential advantages and applications.[1,2] Microreactors are miniaturized reactors that include microchannels whose characteristic dimensions are in the submillimeter range. The reactor miniaturization permits us to proceed reactions under more precisely controlled conditions than conventional macroscale reactors, leading to a possibility of improved yield and selectivity of desired products. An example of precisely controlled reaction conditions using microreactors is suppression of hot spots in highly exothermic reactions, such as phosgene synthesis[3] and direct fluorination[4].

Mixing performance in microreactors is also an essential issue for producing desired products in high yield and selectivity by precisely controlled reactor operation. Yoshida et al. have reviewed the chemical syntheses greatly affected by mixing performance in microreactors.[5] Micromixers, miniaturized mixing devices, are important components of microreactors. Passive and active micromixers have been developed to enhance the mixing performance. Examples of mixing principles of passive mixers are multilamination,[6-8] split and recombination,[9-11] and chaotic advection.[12-14] Examples of mixing principles of active mixers are electronic field,[15] electronic rotator,[16] and ultrasonic.[17] Compared with active mixers, passive mixers have advantages, such as ease of fabrication and maintenance and no need of additional energy.

Computational fluid dynamics (CFD) simulations have been widely used for investigation of microreactors. Using CFD simulations, we can model flows with reaction, diffusion, and convection in microreactors. CFD is especially useful for modeling the mixing and reaction in microreactors since laminar flow due to small reactor dimensions allows us to precisely predict the phenomena in the reactors. CFD simulations are also effective to evaluate reactor performance in microreactors, such as mixing rate and product yield and selectivity, and

Correspondence concerning this article should be addressed to K. Mae at kaz@cheme.kyoto-ac.jp.

identify effects of design factors on the performance. Research instances of passive micromixers using CFD simulations are as follows: Ehlers et al. have studied the progress of the mixing and the product composition for the parallel-competitive reactions in the jetmixer,[18] and Hardt et al. have examined the effects of the mixer chamber geometries on the mixing performance.[19]

Mixing in passive mixers is mainly driven by molecular diffusion because of laminar flow in each channel. The mixing time by molecular diffusion scales with the square of diffusion length. Therefore, to shorten diffusion length is necessary for fast mixing in passive mixers. Mixing operation that reactant fluids are split into many micro fluid segments is often used for this purpose. This operation is used in passive mixers of the first and second mixing principles mentioned previously. In the third type of passive mixers, chaotic mixers, circulatory flow patterns by channel geometry increases interfacial surface area between reactant fluids and thus lead to reduce diffusion length.

In the design of passive mixer using fluid segments to achieve desired mixing performance, sizes and geometry of fluid segments are essential design factors, but design methods of fluid segments have not been established. In this study, we thus aim at developing design methods of fluid segments. In the previous study,[20] we have shown the beneficial effects of feeding reactants at laminated fluid segments into microreactors and the lamination width necessary to achieve desired reactor performance. In most cases, when the conversion of the reactant is the same, the yield and selectivity of the desired product increases with decreasing lamination width. An exception is that the rate constant of the reaction producing the desired product is much smaller than that consuming the desired product, and the order of the former reaction is less than the latter. In this reaction kinetics, the feed with large lamination width shows higher yield of the desired product than the feed with perfectly mixed.

Besides the lamination width, arrangements and shapes can be regarded as geometric design factors of fluid segments when geometry of inlet channels can be changed arbitrarily. The effects of channel geometry on flow pattern and friction factor have been investigated.[21,22] Triangle and rectangle, as well as circle are applied as cross-sectional shapes of channels. The channel geometry is also an important design factor for improving reactor performance. We have, thus, extended the previous study and examined the qualitative effects of the geometric design factors of fluid segments on the mixing performance and the product yield for a series-parallel reaction system.[23] The results have indicated that these factors greatly affect the product yield. The results also mean that mixing rates by molecular diffusion on the plain perpendicular to the axial direction of reactors depend on the geometric design factors. Identifying the quantitative effect of the geometric design factors on the mixing rate by molecular diffusion, and the relative mixing rates to reaction rates is then need for the design of fluid segments to produce desired products in high yield and selectivity.

We introduce two dimensionless numbers that represent effects of the geometric design factors of fluid segments on mixing rate and product yield and selectivity in reactors where reactants are fed with fluid segments. We also devise methods to determine these numbers for a reactor of an arrangement and a cross-sectional shape of fluid segments in the reactor inlet. If these numbers can predict reactor performance regardless of the geometric design factors of fluid segments, we can determine cross-sectional shapes and arrangements of fluid segments giving desired reactor performance using these dimensionless numbers. To investigate effectiveness of these numbers on estimating reactor performance, we compare yields of the desired product of a series-parallel reaction system in a reactor where reactants are fed with fluid segments of an arrangement and a cross-sectional shape with that in the reactor where reactants are fed with fluid segments of rectangular cross sections regularly arranged in 2-D directions using CFD simulations. In this comparison, the two reactors take the same dimensionless numbers. We also discuss effects of the ratio of the rate constants of the reaction system, the mole ratio of reactants, and the laminar flow velocity distribution on the effectiveness of the dimensionless numbers. Through the discussion, we also mention design guidelines for geometry of fluid segments using the two-dimensionless numbers.

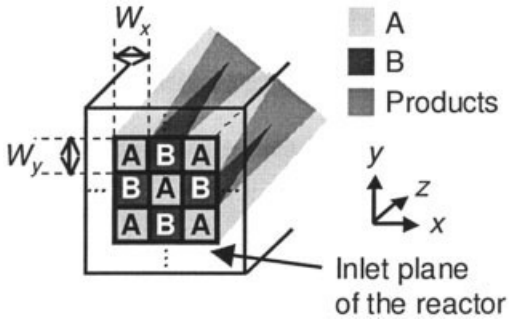

Figure 1. Reactor where reactant fluids are fed with the form of fluid segments.

Definition of Dimensionless Numbers

Derivation of dimensionless numbers

Figure 1 shows a reactor where reactant fluids are fed with the form of fluid segments. First, we introduce assumptions for the reactor. The reactor inlet plane corresponds to the *xy* plain, and the axial direction corresponds to the *z* axis. Reactant fluids for reactants A and B are split into many fluid segments before the inlet plane, and then fed into the reactor. The reactants mutually mix only by molecular diffusion and then react in the reactor. The reaction takes place from the interfaces between each reactant fluid. For simplicity of CFD simulations, channels for splitting reactant fluids into fluid segments are omitted in this study. The reactant fluids are, thus, assumed to be fed into the reactor through the cross section of fluid segments in the reactor inlet plane. We consider cross-sectional shapes and arrangements of fluid segments in the reactor inlet plane as the geometric design factors in this study. In this reactor, cross sections whose characteristic sizes, which relate to diffusion length and will be defined in the next section, are W_x and W_y are arranged regularly in 2-D directions. We also assume that the velocity distribution in the reactor is flat. In actual microreactors, laminar flow velocity distribution develops, but the distribution is approximately flat around the center of the reactor channel. When we assume that a large number of fluid segments are arranged regularly in the inlet plane of the reactor

and deal with the region around the center of the reactor channel, the flat velocity distribution can be a good approximation. This approximation is also useful to identify effects of the design factors on mixing by molecular diffusion, and to elucidate the definition of dimensionless numbers. We also examine the validity of the dimensionless numbers in the reactor with developing velocity distribution of laminar flow in the latter part of this article.

The reaction formulas and the rate equations of a series-parallel reaction system proceeding in the reactor are as follows

$$\left.\begin{array}{ll} A + B \rightarrow R, & r_1 = k_1 C_A C_B \\ B + R \rightarrow S, & r_2 = k_2 C_B C_R \end{array}\right\} \quad (1)$$

where A and B are the reactants and the key components; R is the desired product; S is the byproduct; r_i and k_i are the reaction rate [kmol · m^{-3} · s^{-1}], and the rate constant of the ith reaction [m^3 · kmol^{-1} · s^{-1}], respectively; and C_j is the molar concentration of the component j [kmol · m^{-3}]. When the axial dispersion is negligible, the mass conservation equations for the key components are given by

$$-v_z \frac{\partial C_A}{\partial z} + D_A\left(\frac{\partial^2 C_A}{\partial x^2} + \frac{\partial^2 C_A}{\partial y^2}\right) - k_1 C_A C_B = 0, \quad (2)$$

$$-v_z \frac{\partial C_B}{\partial z} + D_B\left(\frac{\partial^2 C_B}{\partial x^2} + \frac{\partial^2 C_B}{\partial y^2}\right) - (k_1 C_A C_B + k_2 C_B C_R) = 0 \quad (3)$$

where D_j is the diffusion coefficient of the component j [m^2 · s^{-1}]; v_z is the velocity of the reactant fluid flows [m · s^{-1}] and is constant in the whole reactor volume from the assumption of the flat velocity distribution. In the lefthand sides of both equations, the first term represents the convection, the second molecular diffusion, and the third consumption by the reactions. We then transform the above equations into a dimensionless form by the following dimensionless numbers

$$\tau = \frac{D_A}{W_x W_y v_z} z,\ X = \frac{x}{W_x},\ Y = \frac{y}{W_y},$$
$$w = \frac{W_y}{W_x},\ c_A = \frac{C_A}{C_{A0}},\ c_B = \frac{C_B}{C_{B0}},\ c_R = \frac{C_R}{C_{A0}} \quad (4)$$

where C_{j0} is the feed concentration of the component j. The mass conservation equations in a dimensionless form for the key components A and B are

$$-\frac{\partial c_A}{\partial \tau} + \left(w\frac{\partial^2 c_A}{\partial X^2} + w^{-1}\frac{\partial^2 c_A}{\partial Y^2}\right) - \frac{k_1 C_{B0} W_x^2}{D_A} w c_A c_B = 0, \quad (5)$$

$$-\frac{C_{B0}}{C_{A0}}\frac{\partial c_B}{\partial \tau} + \frac{D_B}{D_A}\frac{C_{B0}}{C_{A0}}\left(w\frac{\partial^2 c_B}{\partial X^2} + w^{-1}\frac{\partial^2 c_B}{\partial Y^2}\right) - \frac{k_1 C_{B0} W_x^2}{D_A} w\left(c_A c_B + \frac{k_2}{k_1} c_B c_R\right) = 0 \quad (6)$$

From these equations, dimensionless concentration profiles of the components in the reactor depend on the following dimensionless numbers: C_{B0}/C_{A0}, D_B/D_A, k_2/k_1, $\phi = k_1 C_{B0} W_x^2/D_A$, and w. The dimensionless number ϕ represents the ratio of the reaction rate to the rate of the mixing by molecular diffusion and is called the Damköhler number.[24] When the first three dimensionless numbers are fixed, the profiles can be determined by ϕ and w, which depend on the geometric design factors and are focused on in this article. To determine these two numbers, methods to obtain the characteristic sizes for fluid segments should be established.

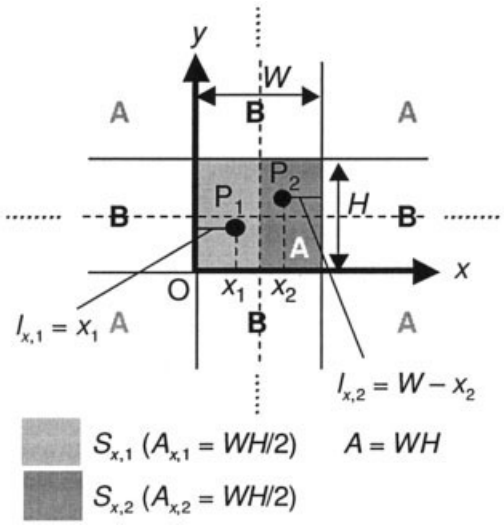

Figure 2. Coordinates and symmetric properties of the rectangle cross section to determine L_i.

Fluid segments are arranged regularly in the two-dimensional directions. The points P_1 and P_2 are placed to determine L_x for this geometric design of fluid segments.

Methods to determine the characteristic sizes and the dimensionless numbers

We then define methods to determine characteristic sizes W_x and W_y for fluid segments so that the dimensionless numbers represent the rate of mixing by molecular diffusion, and the relative rates of reaction to mixing in the reactor. We explain the methods by determining characteristic sizes and dimensionless numbers of a reactor whose fluid segments has a rectangle cross section and are arranged regularly in the 2-D directions shown in Figure 2 as the reference case. The rectangle has the width W and the height H. Here, we assume that W is larger than H. Figure 2 also shows the coordinate and the symmetric properties of the rectangle denoted by the broken lines. This figure is used to determine the characteristic sizes and the dimensionless numbers.

To correlate the characteristic sizes with the diffusion length, we first consider mean diffusion length in each 2-D direction. We regard the shortest distance in the x direction between any point in the segment cross section of a reactant and the interface of the reactants as the diffusion length in this direction. A cross section, whose area is A, has some interfaces, and is divided into domains $S_{x,j}$ where any point takes the common interface as the end point of the diffusion length. In this rectangle, A is equal to WH, and the shape is divided into the two domains $S_{x,1}$ and $S_{x,2}$ by the symmetric property in the x direction. The diffusion length at a point in each domain $S_{x,j}$,

whose cross-sectional area is $A_{x,j}$, is denoted by $l_{x,j}$. In this instance, $A_{x,1} = A_{x,2} = WH/2$. Using the coordinate shown in Figure 2, $l_{x,1}$ is equal to x_1 at the point P_1, and $l_{x,2}$ is equal to $W - x_2$ at the point P_2. The mean diffusion length in this direction for each divided area $L_{x,j}$ is then obtained by integrating $l_{x,j}$ over $S_{x,j}$, and then divided by $A_{x,j}$. Finally, the mean diffusion length for the whole cross section L_x is obtained by area-weighted arithmetic average of $L_{x,j}$. These procedures are expressed by

$$L_{x,j} = \frac{\int\int_{S_{x,j}} l_{x,j}\,dA}{A_{x,j}}, \; L_x = \frac{\sum_{j=1}^{n} A_{x,j}L_{x,j}}{A} \tag{7}$$

Using the symmetric property of the rectangle, we obtain the mean diffusion length in the x direction for this reactor as follows

$$L_{x,j} = L_x = \frac{\int_0^{H/2}\int_0^{W/2} x\,dx\,dy}{A/4} = \frac{W}{4}\,(A = WH) \tag{8}$$

These procedures are repeated for the y direction, and we have the mean diffusion length $L_y = H/4$. From the definition by Eq. 7, $L_{i,j}$ is the first moment of area divided by the area of the domain $S_{i,j}$ and, thus, equal to the distance in the i direction between the center of mass of the domain and the interface of the reactants for the domain.[25]

The mean diffusion length L_i is then correlated with W_i. To equalize the characteristic sizes with the sizes of the rectangle, we define the characteristic sizes as $W_x = 4L_x$ and $W_y = 4L_y$, that is, $W_x = W$ and $W_y = H$ in this instance. Then, we determine the value of w. We can choose the x and y directions arbitrarily. Thus, we take the characteristic size in the direction that has the smaller W_i as the denominator of w. In other words, w is always 1 or more and means the aspect ratio of the mean diffusion lengths in the 2-D directions. In this reactor, $w = W/H$. Therefore, we conclude that $\phi = k_1 C_{B0}(4L_y)^2/D_A = k_1 C_{B0} H^2/D_A$, and $w = W/H$.

When the geometric design factors are changed, more methods to determine the dimensionless numbers are needed. If each cross section has different W_i, we first obtain W_i for each cross section, and then W_i for all cross sections by the area-weighted arithmetic average. Using the methods described above, the characteristic sizes and the dimensionless numbers for a reactor of a cross-sectional shape and an arrangement of fluid segments is determined in the subsequent sections.

Shape

We illustrate calculations of the dimensionless numbers for reactors whose fluid segments take a cross-sectional shape different from the rectangle. Figure 3 shows the right-angled triangle applied as an instance. The cross sections of fluid segments are regularly arranged in 2-D directions as shown in Figure 3a. In Figure 3a, H denotes the height and W denotes the width of the right-angled triangle. We assume that W is larger than H. Here, we call the reactors by the kind of cross-sectional shapes and arrangements of fluid segments, that is, the reactor shown in Figure 3 is referred as the Triangle-2D.

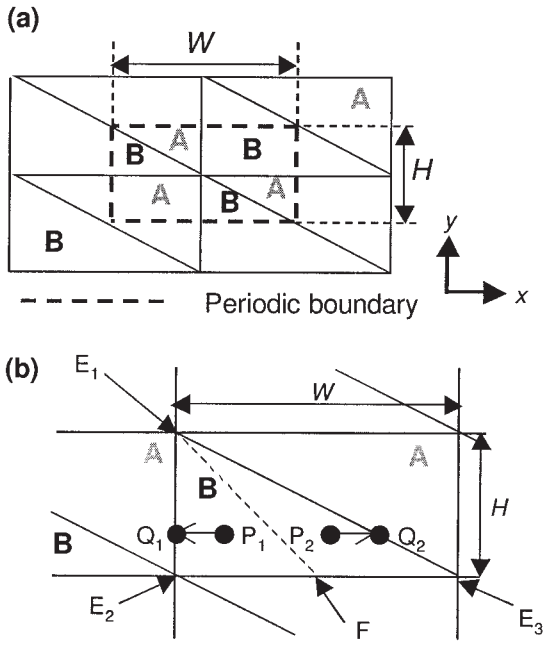

Figure 3. Right-angled triangle as the cross-sectional shape of fluid segments: (a) reactor inlet plane; (b) diffusion length in the *x* direction.

Using Figure 3b, we first calculate L_x. The right-angled triangle $E_1E_2E_3$ is divided into the two domains by the bisector line E_1F. From Eq. 7, $L_{x,j}$ for each domain is equal to the distance in the x direction between the center of mass for E_1FE_2 (P_1) or E_1E_3F (P_2) and the interface of the reactants (Q_1 or Q_2). That is, $L_{x,j}$ for each domain is the length of the segment P_1Q_1 or P_2Q_2. The two domains have the same distances equal to $W/6$, and also have the same area. Thus, we have L_x for the whole cross section, that is, $L_x = (W/6)\times(1/2) + (W/6)\times(1/2) = W/6$. Similarly, we obtain the mean diffusion length in the y direction by only changing W into H, that is, $L_y = H/6$. Therefore, $\phi = k_1 C_{B0}(4L_y)^2/D_A = k_1 C_{B0}(2H/3)^2/D_A = 4k_1 C_{B0} H^2/9D_A$, and $w = W/H$.

Arrangement

Figure 4 shows the reactors having different arrangements of the fluid segments. In these reactors, fluid segments are aligned periodically in one array, two arrays, or three arrays. For the reactors shown in Figure 4a-1–a-3, the cross-sectional shape of fluid segments is the square, whose side length is denoted by H; for the reactors shown in Figure 4b-1–b-3, the cross-sectional shape of fluid segments is the isosceles right-angled rectangle, whose isosceles side length is denoted by H. Each reactor is hereafter called by the name shown in the figures.

The dimensionless numbers for these reactors are then determined. We first obtain the dimensionless numbers for the reactors whose cross-sectional shape of fluid segments is the square shown in Figure 4a-1–a-3. The characteristic sizes in the x direction W_x are equal to H for these three reactors as shown in the previous section. On the other hand, W_y depends on the arrangements of fluid segments. First, for the Rectangle-1

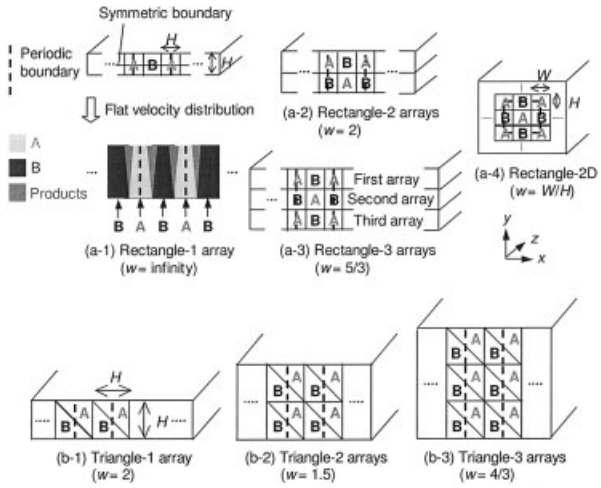

Figure 4. Arrangement of fluid segments: (a) Rectangle (square); (b) Triangle (isosceles right-angled triangle).

array, the reactants cannot diffuse in the y direction since no concentration gradient in this direction is given as shown in Figure 5a. Thus, W_y and w correspond to infinity, and $\phi = k_1 C_{B0} H^2 / D_A$, $w = \infty$. Moreover, when the flat velocity distribution in the y direction is assumed, this reactor can be modeled in the 2-D domain as shown in the bottom of Figure 4a-1. Second, for the Rectangle-2 arrays, the reactants can diffuse upward or downward. Thus, the diffusion length in the y direction becomes twice longer than that of the Rectangle-2-D whose cross-sectional shape is identical as shown in Figure 5b,

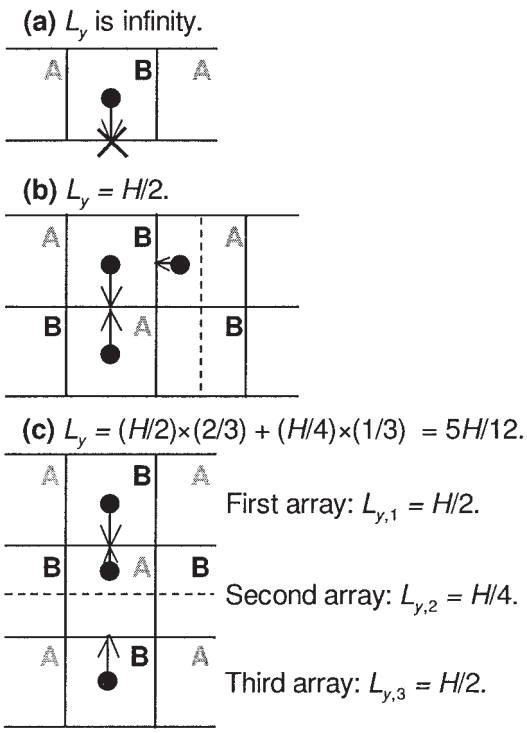

Figure 5. Mean diffusion length in the Rectangle (a) -1 array, (b) -2 arrays, and (c) -3 arrays.

Table 1. Dimensionless Number w of Each Reactor

	w	
Arrangement	Square	Isosceles Right-Angled Triangle
1 array	infinity	2
2 arrays	2	1.5
3 arrays	5/3	4/3
n arrays	$(n + 2)/n \quad (n \geq 2)$	$(n + 1)/n \quad (n \geq 1)$

since the symmetric property shown by the broken line parallel in the x direction in Figure 2 disappears in the Rectangle-2 arrays. Therefore, $L_y = H/2$, which result in $\phi = k_1 C_{B0} H^2 / D_A$, and $w = 2$. Third, for the Rectangle-3 arrays, the reactants in the segments aligned in the first and third arrays can diffuse upward or downward. For these segments, $L_{y,1} = L_{y,3} = H/2$. The diffusion length for the segments in the second array is the same as that for the reactor of 2-D arrangement described in the previous section, that is, $L_{y,2} = H/4$. Figure 5(c) shows the mean diffusion length of reactants in each reactor. Since $L_{y,i}$ for each array is not identical, L_y for this reactor is determined using the procedure explained in the last part of the preceding section. Hence, $L_y = (H/2)\times(2/3) + (H/4)\times(1/3) = 5H/12$, and $W_y = 4L_y = 5H/3$. We conclude that $\phi = k_1 C_{B0} H^2 / D_A$, and that $w = 5/3$.

Extending to the n-array arrangement ($n \geq 2$), L_y for the first and nth array is $H/4$ and for the other $n - 2$ arrays is $H/2$. Therefore,

$$L_y = \frac{H}{2}\frac{2}{n} + \frac{H}{4}\frac{n-2}{n} = \frac{n+2}{4n}H, \; W_y = \frac{n+2}{n}H \quad (n \geq 2) \tag{9}$$

When n is infinity, $L_y = H/2$, and $W_y = H$. They are equal to those for the Rectangle-2D of the square cross section whose side length is H ($W = H$ in Figure 4a-4).

When the cross-sectional shape of fluid segments is the isosceles right-angled rectangle, the dimensionless numbers can be determined similarly. For all reactors shown in Figure 4b-1–b-3, $\phi = 4k_1 C_{B0} H^2 / 9D_A$. Only w depends on the arrangements of fluid segments. Table 1 summarizes the dimensionless number w of each reactor shown in Figure 4a-1–a-3 and b-1–b-3.

Methods of CFD Simulations

First, the settings for all CFD simulations of this study are explained. We simulated the mixing by molecular diffusion, reaction, and flow in reactors of various arrangements and shapes of fluid segments that will be mentioned in the subsequent sections. The reaction formulas, and the rate equations of the multiple reactions proceeding in the reactors are as follows

$$\left.\begin{aligned} A + B &\rightarrow R, \quad r_1 = k_1 C_A C_B \\ B + R &\rightarrow S, \quad r_2 = k_2 C_B C_R \end{aligned}\right\} \tag{10}$$

where A and B are the reactants; R is the desired product; S is the byproduct; r_i and k_i are the reaction rate [kmol · m^{-3} · s^{-1}], and the rate constant of the ith reaction [m^3 · kmol^{-1} · s^{-1}], respectively; and C_j is the molar concentration of the component j. The reactants were assumed to react isothermally, and

Table 2. Cross-Sectional Sizes of Fluid Segments in the Rectangle- and the Triangle-2D

Rectangle-2D				Triangle-2D			
ϕ	w	H [μm]	W [μm]	ϕ	w	H [μm]	W [μm]
10^1	1	32	32	10^1	1	47	47
10^1	2	32	63	10^1	2	47	95
10^1	4	32	126	10^1	4	47	190
10^1	8	32	253	10^1	8	47	379
10^2	1	100	100	10^2	1	150	150
10^3	1	316	316	10^3	1	474	474
10^3	2	316	632	10^3	2	474	948
10^3	4	316	1265	10^3	4	474	1897
10^3	8	316	2530	10^3	8	474	3795
10^4	1	1000	1000	10^4	1	1500	1500

the rate constants were fixed at $k_1 = 1\ \mathrm{m^3 \cdot kmol^{-1} \cdot s^{-1}}$ and $k_2/k_1 = 0.1$ unless otherwise noted. The initial concentrations of the reactants were as follows: $C_{B0} = 10\ \mathrm{kmol^{-1} \cdot m^3}$; $C_{B0}/C_{A0} = 2$ unless otherwise noted. The diffusion coefficient of every component D_j was assumed to be $10^{-9}\ \mathrm{m^2 \cdot s^{-1}}$, which is the typical order of the diffusion coefficient for liquid phase reactions. The physical properties of the two reactant fluids are as follows: the density is 1,000 kg/m^3, and the viscosity is 0.001 Pa·s. The inlet velocity of the reactant fluids u was fixed at $0.001\ \mathrm{m \cdot s^{-1}}$, and the flow in the reactors has flat velocity distribution unless otherwise stated. The flat velocity distribution is obtained by setting the share stress on the reactor wall equal to zero. The reactor length L was set at 1 cm for $\phi = 10^1$, 10^2 and at 10 cm for $\phi = 10^3$, 10^4, that is, the mean residence time of the reactants in the reactors τ was 10 s for $\phi = 10^1$, 10^2 and 100 s for $\phi = 10^3$, 10^4. The vessel dispersion number D_j/uL is equal to 10^{-4} or less, and, thus, the influence of the axial dispersion is negligible.[26] In general, values of u and L are larger that those shown above in microreactors, especially liquid phase reactions. Therefore, the assumption on the axial dispersion is reasonable.

A commercial CFD code Fluent 6.2.16 was used for CFD simulations. This code solves mass, momentum, and energy conservation equations by the control volume method.[27] The laminar flow and the finite-rate model were applied. The SIMPLE algorithm was used to solve pressure-velocity coupling equation. The second-order upwind scheme was used to solve mass and momentum conservation equations. We monitored the mass-average mole fraction of the reactant A in the cross section of the reactor outlet in each iteration and considered the solution converged when the four significant digits of the values between two successive iterations remain unchanged. The residuals of the velocity, and the concentration of the components were also monitored, and the values were less than 10^{-4} when we considered the solution to be converged. The discretization method of the simulation domain is mentioned in the subsequent sections. We confirmed that the solutions of the CFD simulations are independent of the further increase in the number of mesh elements.

Using the settings mentioned previously and the geometric design factors explained in the following sections, we conducted the CFD simulations to obtain concentration profiles of the components in the reactors, and then calculated relations between the yield of the desired product R, Y_R, and the conversion of the reactant A, x_A, in the reactors as a reactor performance measure. These relations were obtained from the mass-weighted average concentration of each component on the plane perpendicular to the axial direction at each axial position. In the reaction system shown by Eq. 10, Y_R increases with enhancing mixing rate. At the same conversion of A, higher yield of R is equivalent to higher selectivity of R. Thus, comparisons of Y_R in reactors of several combinations of the geometric design factors of fluid segments also mean comparisons of mixing rates and selectivities of R.

Shape

For the cross-sectional shape of fluid segments, we investigated the effectiveness of the dimensionless numbers on predicting reactor performance. In other words, we compared the yield of R in the reactors taking the same dimensionless numbers but the different cross-sectional shapes of fluid segments. The rectangle shown in Figure 4a-4 and the right-angled triangle shown in Figure 3 were applied as the cross-sectional shapes. The fluid segments for the reactors of both shapes were regularly arranged in 2-D directions. First, the yield of R in the reactors of the two cross-sectional shapes of fluid segments were calculated with changing ϕ and fixed w. These dimensionless numbers are changed by the sizes of the cross section of fluid segments as shown in Table 2. The sizes H and W in this table correspond to the same sizes in Figures 3 and 4a-4. The dimensionless number ϕ was changed from 10^1 to 10^4, and w was fixed at unity. In this study, influence of the ratio k_2/k_1 was also examined. The change in k_2/k_1 is a case study of a different reaction system. The same simulations only changing the value of k_2/k_1 into 10 with fixed k_1 at $1\ \mathrm{m^3 \cdot kmol^{-1} \cdot s^{-1}}$ were repeated. We also examined effects of C_{B0}/C_{A0} on the validity of the dimensionless numbers to represent the performance of mixing by molecular diffusion. The same simulations only changing the value of C_{B0}/C_{A0} into 0.5 with fixed k_1 at $1\ \mathrm{m^3 \cdot kmol^{-1} \cdot s^{-1}}$ were conducted ($k_2/k_1 = 0.1$).

Second, effects of w were examined. The applied values of w were 1, 2, 4, or 8. In this study, ϕ was fixed at 10^1 or 10^3, relatively close to diffusion controlled conditions. Table 2 also shows the cross-sectional sizes of fluid segments for the Rectangle-and the Triangle-2D for each set of the dimensionless numbers applied in this study.

Since we assume that a large number of fluid segments are arranged regularly in the inlet plane of the reactor and deal with the region around the center of the reactor channel, we applied the periodic boundary conditions shown in Figure 3a and 4a-4. The simulation domains for the reactors of both shapes were the volumes surrounded by the periodic boundaries. Effects of the reactor walls of the vertical and horizontal sides are ne-

Table 3. Grid Elements for Discretization of Each Simulation Domain

Reactor	ϕ	w	Shape of Grid Elements	Number of Grid Elements
Rectangle-2D	10^1	1, 2, 4, 8	Cuboid	80,000
Rectangle-2D	10^2	1	Cuboid	80,000
Rectangle-2D	10^3	1, 2, 4, 8	Cuboid	240,000
Rectangle-2D	10^4	1	Cuboid	640,000
Triangle-2D	10^1	1, 2, 4, 8	Cuboid, Hexahedron	85,600
Triangle-2D	10^2	1	Cuboid, Hexahedron	85,600
Triangle-2D	10^3	1, 2, 4, 8	Cuboid, Hexahedron	256,800
Triangle-2D	10^4	1	Cuboid, Hexahedron	681,600

glected in the simulations. Table 3 summarizes the shape and the number of grid elements for the discreticization of each simulation domain.

Arrangement

We investigated effects of the fluid segment arrangements on product distribution when ϕ is equal to 10^1 or 10^3. When ϕ was fixed at 10^3, the side length of the square cross section of each segment for the reactors shown in Figure 4a-1–a-3 was 316 μm; the isosceles side length of the isosceles right-angled triangle shown in Figure 4b-1–b-3 was 474 μm. When ϕ was fixed at 10^1, the side length of the square cross section was 32 μm; the isosceles side length of the isosceles right-angled triangle was 47 μm.

When $\phi = 10^3$, we adjusted the cross-sectional size for the Rectangle-2D shown in Figure 4a-4 so that this reactor and each reactor shown in Figure 4a-1–a-3 and b-1–b-3 have the same dimensionless numbers. We then compared the yield of R in each pair of reactors taking the same dimensionless numbers but the different arrangements of fluid segments to examine the validity of these dimensionless numbers on estimating reactor performance when arrangements of fluid segments are changed. Table 4 shows the adjusted sizes of the rectangle for the Rectangle-2D. The sizes H and W correspond to the sizes denoted by the same letters in Figure 4a-4. The definite value of w for the Rectangle-1 array is infinity. The corresponding side length of the longer side of the rectangle in the Rectangle-2D is also infinity. However, such size is inapplicable.

Table 4. Adjusted Rectangular Sizes of Fluid Segments in the Rectangle-2D

$\phi = 10^3$			
Compared Reactor	H [μm]	W [μm]	$w = W/H$
Rectangle-1 array	316	5056	16
Rectangle-2 arrays	316	632	2
Rectangle-3 arrays	316	527	5/3
Triangle-1 array	316	632	2
Triangle-2 arrays	316	474	1.5
Triangle-3 arrays	316	422	4/3
$\phi = 10^1$			
Compared Reactor	H [μm]	W [μm]	$w = W/H$
Rectangle-1 array	32	506	16
Rectangle-2 arrays	32	63	2
Rectangle-3 arrays	32	53	5/3
Triangle-1 array	32	63	2
Triangle-2 arrays	32	47	1.5
Triangle-3 arrays	32	42	4/3

Table 5. Grid Elements for Discretization of Each Simulation Domain

Reactor	ϕ	Grid Shape	Number of Grid Elements
Rectangle-1 array (2D)	10^1	Rectangle	8,000
Rectangle-1 array (2D)	10^3	Rectangle	8,000
Rectangle-1 array (3D)	10^1	Cuboid	40,000
Rectangle-1 array (3D)	10^3	Cuboid	40,000
Rectangle-2 arrays	10^1	Cuboid	80,000
Rectangle-2 arrays	10^3	Cuboid	240,000
Rectangle-3 arrays	10^1	Cuboid	120,000
Rectangle-3 arrays	10^3	Cuboid	360,000
Rectangle-2D	10^3	Cuboid	240,000
Triangle-1 array	10^1	Cuboid, Hexahedron	56,800
Triangle-1 array	10^3	Cuboid, Hexahedron	108,000
Triangle-2 arrays	10^1	Cuboid, Hexahedron	84,800
Triangle-2 arrays	10^3	Cuboid, Hexahedron	169,200
Triangle-3 arrays	10^1	Cuboid, Hexahedron	127,200
Triangle-3 arrays	10^3	Cuboid, Hexahedron	253,800

Thus, we set at $w = 16$ as a sufficiently large value for the Rectangle-2D in the comparison of the yield of R between the Rectangle-1 array and the Rectangle-2D.

The dimensionless numbers ϕ and w are derived under the approximation of the flat velocity distribution, and the velocity distribution in the reactor described earlier is also flat. Laminar velocity distribution, however, develops in actual microreactors. To use these numbers in the design of actual microreactors, we need to know effects of the velocity distribution on mixing and product distribution. We then examined the effects of the developing velocity distribution on the design of fluid segments using the dimensionless numbers. Besides the flat velocity distribution, we, thus, applied the laminar velocity distribution in the reactors shown in Figure 4a-1–a-3 and b-1–b-3 by setting the no-slip boundary condition on the reactor walls. The flat velocity distribution at the reactor inlet and the sizes of fluid segments shown in Table 4 remained unchanged in this study. The laminar velocity distribution thus develops after the reactor inlet. We compared mixing performance and product yield in each reactor of the two velocity distributions.

Since we assume that a large number of fluid segments are arranged periodically in the inlet plane of each reactor and deal with the region around the center of the reactor channel in the horizontal direction, the periodic boundary conditions shown in Figure 4 were applied in the simulations. The simulation domain for the Rectangle-1 array is 2-D as shown in the top of Figure 4a-1 when the velocity distribution in the y direction is flat and 3-D as shown in the bottom of Figure 4a-1. when the laminar velocity distribution develops in the reactor. The domains for the Triangle-1 array, the Rectangle- and the Triangle-2 arrays, and the Rectangle- and the Triangle-3 arrays were the volume surrounded by the periodic boundaries, and the walls of the reactor. Effects of the reactor walls of the vertical sides were neglected in the simulations for the reactors mentioned previously. The domain for the Rectangle-2D was the volume surrounded by the periodic boundaries. The effects of the reactor walls of the vertical and horizontal sides are neglected in the simulations for the Rectangle-2D. Table 5 summarizes the shape and the number of mesh elements for the discreticization of each simulation domain.

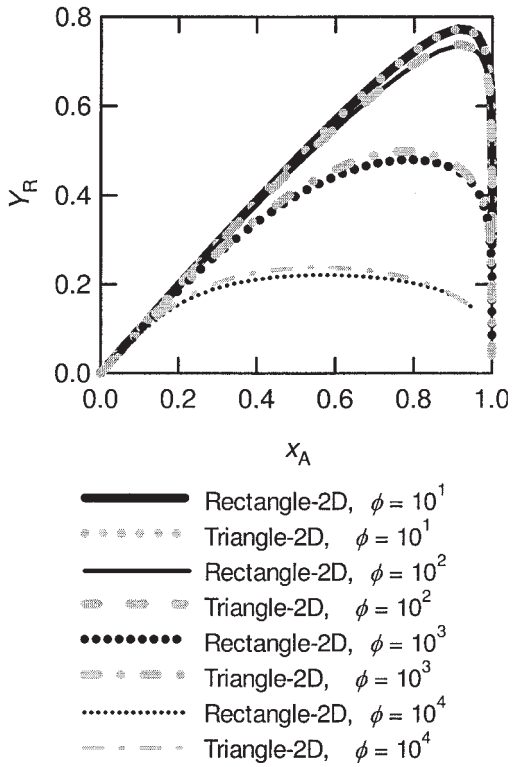

Figure 6. Influences of ϕ on Y_R for the Rectangle-2D and the Triangle-2D.

$C_{B0}/C_{A0} = 2$; $k_2/k_1 = 0.1$; $w = 1$.

Results and Discussion

Effects of ϕ for the two shapes

Figure 6 shows the effect of ϕ (the ratio of the reaction rate to the rate of the mixing by molecular diffusion) for the Rectangle-2D and the Triangle-2D on Y_R when w is fixed at unity. The dimensionless number ϕ is changed by the size of the cross section of the fluid segments shown in Table 2. When ϕ is fixed, the reactor length also defined as mentioned in the first part of "Methods of CFD simulations." The relations between Y_R and x_A are calculated from the value of mass-weighted average of mass fraction of A and R on the plain perpendicular to the axial direction at each axial position in each reactor of a set of the dimensionless numbers. Each line of Y_R vs. x_A is obtained from the result of each simulation for a reactor of a set of the dimensionless numbers. The relations between Y_R and ϕ approximately correspond. When $\phi = 10^4$, the difference in maximum Y_R for the two reactors is the largest, and the Triangle-2D gives 8% higher maximum Y_R than the Rectangle-2D. The dimensionless number ϕ thus, serves as the index for the estimate of the mixing rate, and the product yield and selectivity when $w = 1$. We can also identify whether reactions proceed under reaction-controlled conditions from the value of ϕ. When $\phi = 10^1$, the yield of R in the reactors of both cross-sectional shapes agree with that in the reaction controlled case.[26] Small values of ϕ mean that relative rates of reaction to mixing by molecular diffusion are slow. Therefore, $\phi = 10^1$ is the threshold for reaction controlled conditions when w is fixed at unity in this reaction system. Using the threshold value of ϕ, we can determine maximum sizes of fluid segments achieving ideal mixing for reaction controlled conditions and avoid designing smaller fluid segments and, thus, smaller sizes of channels producing such fluid segments than necessary for achieving ideal mixing. That is, structure of the order of micrometer should be used only in the part of the reactor where the size is really needed. Avoiding smaller channel sizes than necessary is desirable, since pressure drop increases with reducing the sizes.

When $\phi = 10^4$, Y_R is much lower than that under reaction controlled conditions. In design of fluid segments, mixing operation at this value of ϕ is impractical. However, we can also use the results in Figure 6 to determine mixing performance with reaction system whose rate constants are known and take very large values. In a study to determine mixing rate of a mixing operation using a reaction system of high values of rate constants, the operation could be performed under the condition at $\phi = 10^4$ due to the high values of the rate constants. Moreover, when we study a very fast reaction system, and its rate constants are unknown, we could mix reactants under the corresponding condition where ϕ is as large as 10^4.

Moreover, we discuss the effect of the ratio of the rate constants k_2/k_1. Figure 7 shows the corresponding results of Figure 6 with only changing the value of k_2/k_1 from 0.1 into 10 with fixed k_1. For this value of k_2/k_1, the relations between Y_R and ϕ for the Rectangle-2D also agree well with that for the Triangle-2D. For reactors of both cross-sectional shapes of fluid segments, the conversion of A giving the highest Y_R for $k_2/k_1 = 10$ is lower than that for $k_2/k_1 = 0.1$. Thus, low

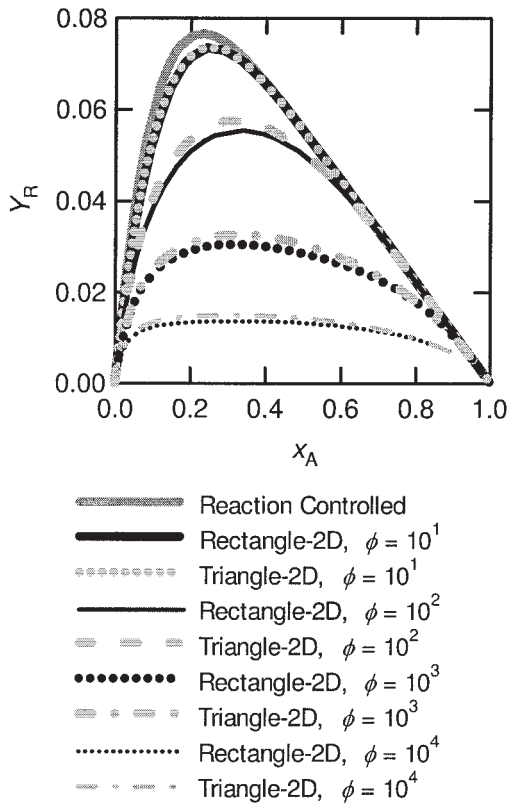

Figure 7. Influences of ϕ on Y_R for the Rectangle-2D and the Triangle-2D.

$k_2/k_1 = 10$; $C_{B0}/C_{A0} = 2$; $w = 1$.

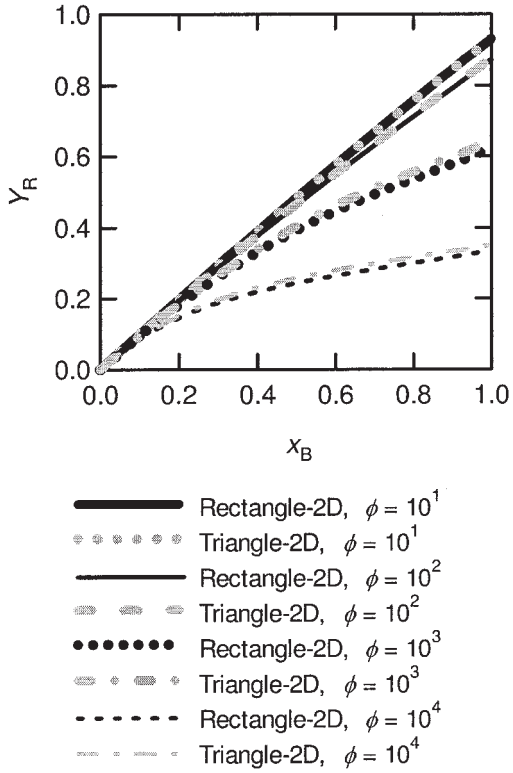

Figure 8. Influences of ϕ on Y_R for the Rectangle-2D and the Triangle-2D.

$C_{B0}/C_{A0} = 0.5$; $k_2/k_1 = 0.1$; $w = 1$.

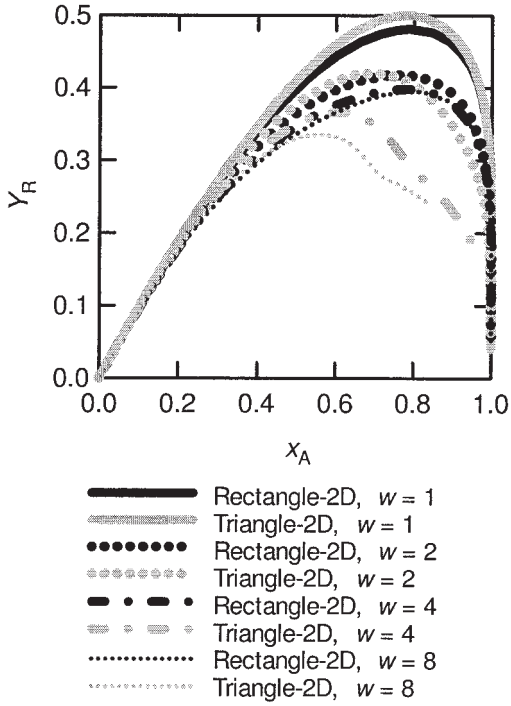

Figure 9. Influences of w on Y_R for the Rectangle-2D and the Triangle-2D.

$\phi = 10^3$.

conversions of A given by short residence times are favorable to achieve high yields and selectivities of R. The threshold of ϕ for reaction controlled conditions, however, depends on k_2/k_1. When $\phi = 10^1$, the yield of R for both reactors are lower than that under reaction controlled conditions. For achieving reaction controlled conditions, a smaller value of ϕ is needed in this reaction kinetics. In other words, the relative mixing rate to reaction rate required to perform ideal mixing rises with increasing k_2/k_1. The reason can be explained as follows. When k_2/k_1 is large, the first reaction of Eq. 10 controls the reaction rates of the whole reaction system. The diffusion length between A and B is longer than that between B and R, since R mainly exists around interfaces between A and B. The first reaction of Eq. 10 is, thus, strongly affected by the mixing. Consequently, for achieving reaction controlled conditions, importance of fast mixing of the reactants rises with increasing k_2/k_1.

In the previous sections, the mole ratio of the reactants C_{B0}/C_{A0} have been fixed at 2. We then changed the value of C_{B0}/C_{A0}. Figure 8 shows the corresponding results of Figure 6 with only changing the value of C_{B0}/C_{A0} from 2 into 0.5 with $k_2/k_1 = 0.1$ and $w = 1$. In this value of C_{B0}/C_{A0}, B is the limiting component. We, thus, take the conversion of B, x_B, as the variable of the x axis in this figure. The relations of the dimensionless numbers and Y_R for the reactors of both cross-sectional shapes of fluid segments are similar to those shown in Figure 6. When $\phi = 10^1$, the yields of R in the reactors of both cross-sectional shapes of fluid segments agree with that under reaction controlled conditions.

Effects of w for the two shapes

Figure 9 shows the yield of R in the reactors of the two cross-sectional shapes for each w (the aspect ratio of the mean diffusion lengths in the 2D directions) with fixed ϕ at 10^1. The maximum yield of R for the Triangle-2D is higher than that for the Rectangle when $w = 1$ and 2. On the other hand, when w is larger than 2, the Rectangle-2D gives higher maximum yield of R than the Triangle-2D. The difference in Y_R for the two reactors is especially large at high conversion of A and increases with enlarging fluid segments in the x direction.

The effect of w on the product yield depends on the cross-sectional shapes because the transition of the concentration profiles of the reactants along with the mixing by molecular diffusion in each reactor is different. Figure 10 shows the contour plots of C_A/C_{A0} in the reactors. In the Rectangle-2D,

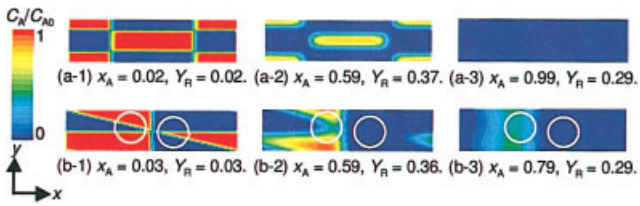

Figure 10. Mixing by molecular diffusion in the reactor of each cross-sectional shape: (a) Rectangle-2D; (b) Triangle-2D.

The figures show the contour plots of C_A/C_{A0} at $z = 0.0001$ m ((a-1) and (b-1)), $z = 0.004$ m ((a-2) and (b-2)), and $z = 0.02$ m ((a-3) and (b-3)). $\phi = 10^3$, and $w = 4$. [Color figure can be viewed in the online issue, which is available at www.interscience.wiley.com.]

when w is 4 or larger, the mixing by the molecular diffusion in the direction giving the shorter mean diffusion length, namely the y direction in Figure 8, proceeds much faster than that in the x direction. The height of the rectangular cross section and the diffusion length in the y direction are uniform at any x coordinate. Thus, the diffusion in the y direction at any x coordinate except for the both ends of the rectangle completes at the same time, and the mixing in the whole reactor volume also completes. At the both ends, the diffusion in the x direction also affects the mixing rate, and the mixing completes earlier than the other reactor volume. Thus, the further increase in w for the Rectangle-2D with fixed ϕ has minor importance on the mixing rate in the whole reactor volume and, thus, the yield of R. For the Triangle-2D, the influence of w on the reactor performance is greater than that for the Rectangle-2D. In this reactor, the diffusion length in the y direction depends on the position in the x direction. The reactant A or B in the area circled in Figure 10b has shorter diffusion length and completes the mixing and the reactions earlier than that in the other area. Beside the circled area, large portion of the counterpart reactant of the first reaction in Eq. 10 remains unreacted. Figure 10b-3 shows that the unreacted reactants are detached in the x direction and have a long diffusion length. The distance between the remained reactants in the x direction is enlarged with increase in w. Thus, the mixing between the remained reactants at high value of w proceeds slowly and results in low Y_R at high conversion of A. Consequently, w for the Triangle-2D should be close to unity for fast mixing. Besides the decrease in the product yield, since fabricating channels to produce fluid segments whose cross-sectional shape is the right-angled triangle of a high value of w is difficult, such fluid segments are impracticable. We can also conclude that rectangles as cross-sectional shapes of fluid segments are more favorable than triangles from the viewpoint that the mixing proceeds homogeneously in the cross-sectional plane of reactors especially when w takes large values.

We then discuss the results of $\phi = 10^1$. Figure 11 shows the corresponding results of Figure 9 with only changing the value of ϕ into 10^1. As mentioned in the previous section, the value of w has minor importance on mixing performance and thus Y_R in the Rectangle-2D at $\phi = 10^1$. The yield of R is unchanged with increasing w. On the other hand, Y_R for the Triangle-2D decreases with increasing w. This tendency is consistent with that discussed earlier. The effect of w is, however, smaller than that when $\phi = 10^3$. Therefore, to achieve reaction controlled conditions, we need only pay attention to the value of ϕ when we choose rectangle as the cross section of fluid segments. In contrast, we need pay attention to the value of w as well as that of ϕ when we choose triangle as the cross-sectional shape.

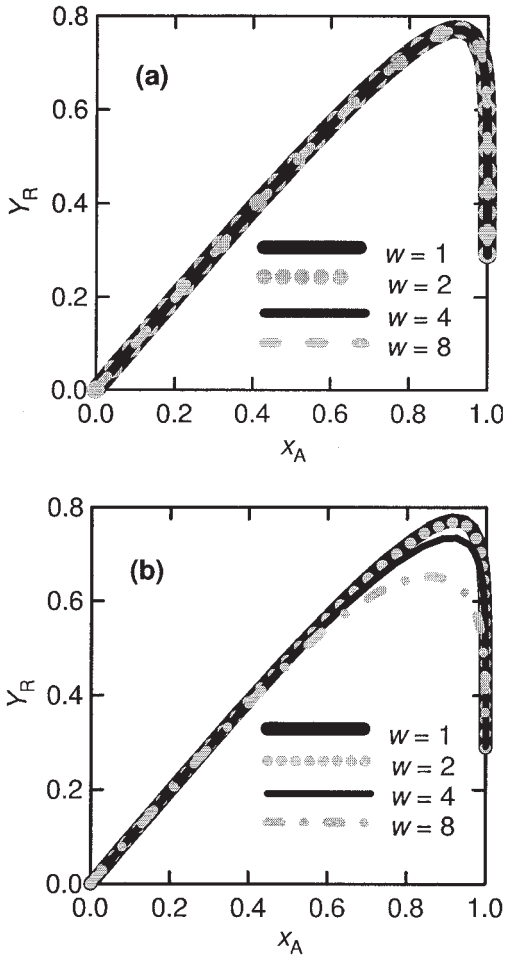

Figure 11. Influences of w on Y_R for (a) the Rectangle-2D and (b) the Triangle-2D.

$\phi = 10^1$.

Arrangement

Figure 12 shows the relation between Y_R and x_A in the reactors where the reactants are given by the various arrangements of fluid segments shown in Figure 4. When the cross-sectional shape of fluid segments is the square, the results show that the yield of R in each reactor shown in Figure 4a-1–a-3 agrees well with that in the Rectangle-2D of the corresponding dimensionless numbers. When the Rectangle-2D takes the value of $w = 16$, this reactor gives the comparable yields of R in the reactors to that in the Rectangle-1 array. In the Rectangle-2D whose w is 16, the mixing in the Rectangle-2D mainly proceeds by the molecular diffusion in the direction giving the shorter diffusion length, namely, the y direction, and the influence of the further increase in w on the mixing rate and the product yield is negligible. Thus, we can infer the reactor performance of the Rectangle-2D of $w = 16$ is equivalent to that of $w = \infty$. Therefore, w can represent the effect of the segment arrangement of square cross sections on the product yield. Using ϕ and w, we can estimate product yields in a reactor whose fluid segments have square cross section of a side length and are arranged in an arrangement.

When the cross-sectional shape of fluid segments is the isosceles right-angled rectangle, the difference in the yield of R between each reactor shown in Figure 4b-1–b-3, and the Rectangle-2D of the corresponding dimensionless numbers is larger that between each reactor shown in Figure 4a-1–a-3, and the Rectangle-2D. The Triangle-3 arrays shows higher maximum Y_R than the Rectangle-2D of the corresponding dimensionless number. On the other hand, the Triangle-1 array and -2 arrays gives lower maximum Y_R than the Rectangle-2D. The tendency that the Triangle of each arrangement of fluid segments gives the lower Y_R than that for the Rectangle-2D especially at high conversion of A is similar to that in the preceding discussion of the effect of w for each cross-sectional shapes. These results

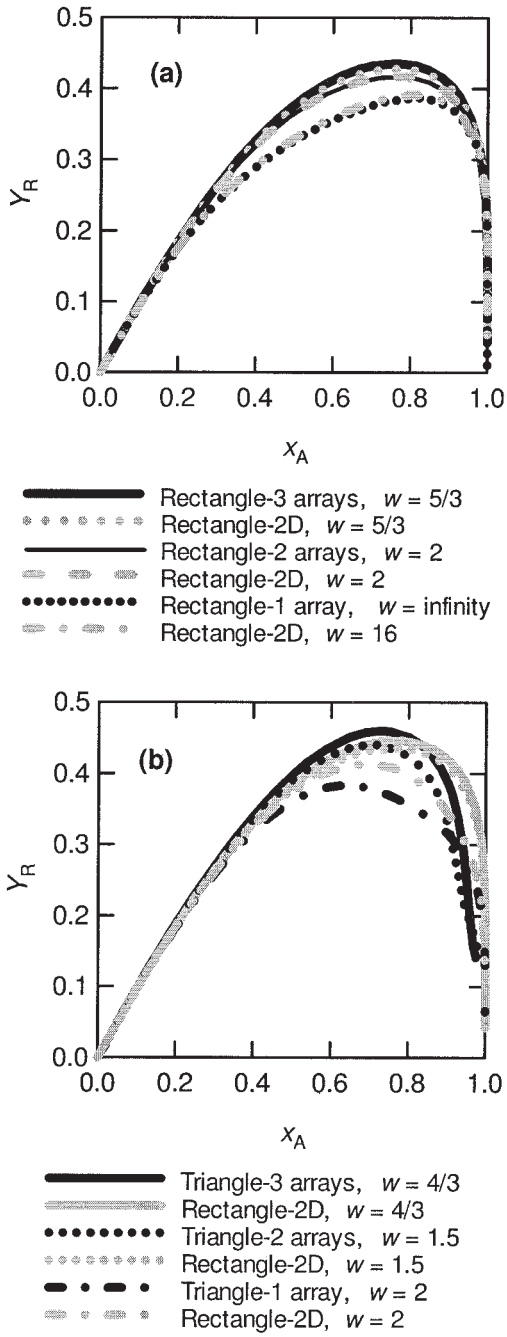

Figure 12. Effects of the arrangements on the yield of R in the reactors: (a) Rectangle; (b) Triangle.
$\phi = 10^3$.

also indicate that the dependence of the reactor performance on w for the Triangle is greater than that for the Rectangle. Thus, multiple-array arrangement of the Triangle is more important than that of the Rectangle to reduce the value of w and, thus, to improve mixing rate.

We then discuss the results of $\phi = 10^1$. Figure 13 shows the corresponding results of Figure 12 with only changing the value of ϕ into 10^1. The yield of R is unchanged by the arrangement and cross-sectional shapes of fluid segments in this value of ϕ. As shown in Figure 11, Y_R in the Rectangle-2D is independent of w, and that in the Triangle-2D is comparable to that under reaction controlled conditions when w is equal to 2 or less. Therefore, we can infer the results shown in Figure 13 from the value of the dimensionless numbers of each reactor. In these instances, regardless of arrangement of fluid segments, the yield of R is identical to that under reaction controlled conditions. We thus need other viewpoint to determine the geometric design factors of fluid segments. One of the viewpoint is ease of fabrication of channel geometries for splitting reactant fluids into fluid segments. Channel geometries for one array arrangement and rectangle cross-section is the easiest to realize in the examples of the arrangements and the cross-sectional shapes of fluid segments. These arrangement and cross-sectional shape are seen in the interdigital mixer[6] and superfocus micromixer[8].

Effects of the laminar velocity distribution

We then discuss effects of the laminar velocity distribution on the mixing and the yield of the desired product. The velocity distribution given at the reactor inlet is flat. Entrance length, L_e, is, thus, needed for developing the laminar velocity distribution

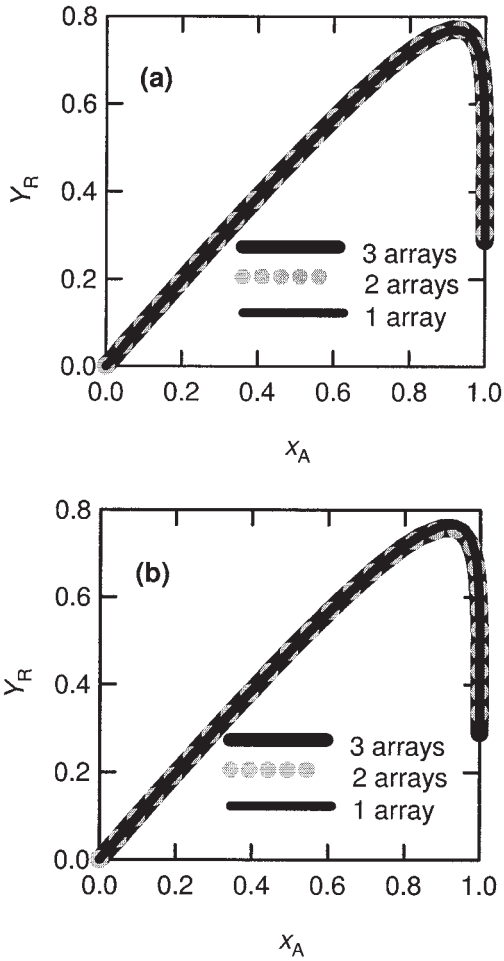

Figure 13. Effects of the arrangements on the yield of R in the reactors: (a) Rectangle; (b) Triangle.
$\phi = 10^1$.

when the no-slip boundary condition is applied on the reactor walls. This length is expressed by

$$L_e/D = 0.379 \exp(-1.48\,\mathrm{Re}) + 0.0550\,\mathrm{Re} + 0.260 \quad (11)$$

where D and Re are the hydraulic diameter of the reactor channel and the Reynolds number,[28] respectively.[28] The entrance lengths obtained by Eq. 11 approximately correspond to the results of the CFD simulations. Compared among the reactors of $\phi = 10^3$, the length of the Triangle-3 arrays is the longest, 1.9×10^{-3} m ($D = 2.8 \times 10^{-3}$ m, and Re = 2.8), and the length of the Rectangle-1 array is the shortest, 4.0×10^{-4} m ($D = 6.3 \times 10^{-4}$ m, and Re = 0.63). For the Triangle-3 arrays, the conversion of A is 0.58 at $z = 1.9 \times 10^{-3}$ m. For the Rectangle-1 array, the conversion of A is 0.10 at $z = 4.0 \times 10^{-4}$ m. These results show that some extent of the reactions proceeds within the entrance length.

Figure 14 shows Y_R in the reactors shown in Figure 4, with the flat or the laminar velocity distribution in the y direction when $\phi = 10^3$. The yield of R for the Rectangle-1 array remains unchanged by applying the laminar velocity distribution. In this reactor, no concentration gradient is given in the y direction. Thus, the effect of the velocity distribution has minor importance. The other reactors with the laminar velocity distribution in the y direction show the higher yield of R than those with the flat velocity distribution, since the reactant fluids gather in the middle of the reactor channel in the y direction along with developing the velocity distribution. Figure 15 illustrates the effect of the laminar velocity distribution on the concentration profile of the reactant A for reactors of 3-array arrangement and both cross-sectional shape. The development of the velocity distribution causes the contraction of the fluid segment aligned in the second array. The fluid segment contraction by developing the laminar velocity distribution results in the same effect of reducing the height of the fluid segment and, thus, w when the flat velocity distribution is applied. For instance, the Rectangle-3 arrays ($\phi = 10^3$ and $w = 5/3$) with the laminar velocity distribution gives the comparable Y_R of the Rectangle-2D ($\phi = 10^3$ and $w = 1$) with the flat velocity distribution. The results also indicate that the reactor performance of a reactor of a set of the dimensionless numbers with the laminar velocity distribution is comparable to or higher than that by the estimate using the reactor of the identical dimensionless numbers with the flat velocity distribution.

Figure 16 shows the effect of the laminar velocity distribution on the product yield in the Rectangle-3 arrays, and the Triangle-1 array when $\phi = 10^1$. We choose these reactors because Y_R of these reactors are strongly affected by the velocity distribution as shown in Figure 14. In this value of ϕ, Y_R for these reactors are independent of the velocity distribution. We also confirmed that Y_R of the reactors of other arrangements and cross-sectional shapes are independent of the velocity distribution when $\phi = 10^1$. These results indicate that the threshold value of ϕ for reaction controlled conditions is also independent of the velocity distribution, and that the approximation of the flat velocity distribution is, thus, reasonable especially when reaction controlled conditions are achieved. Therefore, we can design fluid segments for microreactors with laminar flow velocity distribution using the threshold value of the dimensionless numbers for reaction controlled conditions derived from the approximation of the flat velocity distribution.

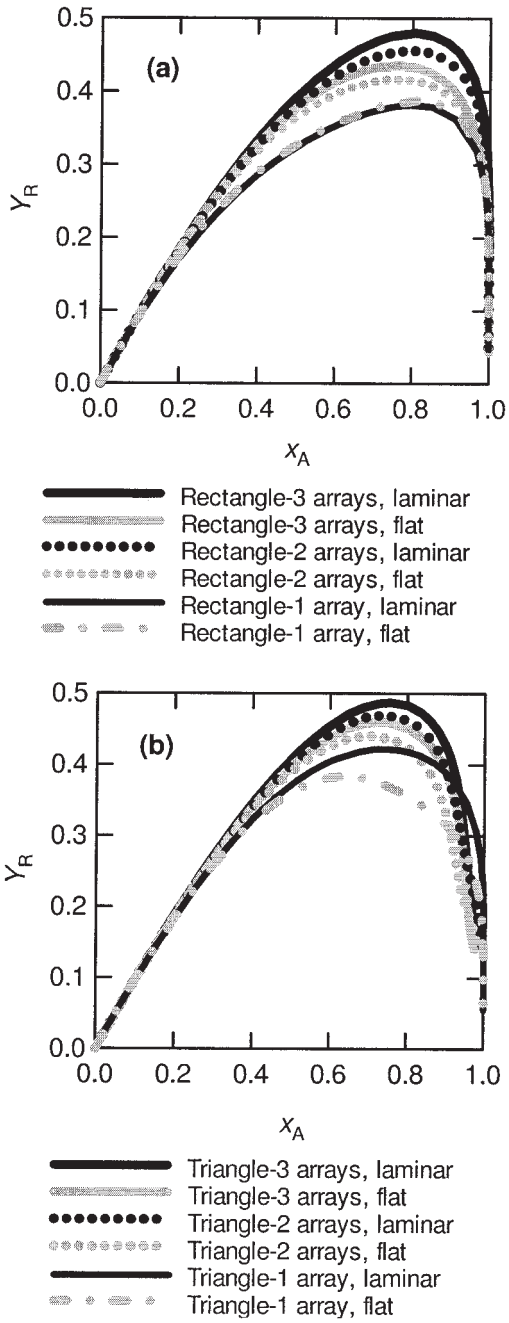

Figure 14. Effect of the laminar velocity distribution on the product yield: (a) Rectangle; (b) Triangle.
$\phi = 10^3$.

Conclusions

In microreactors, the mixing operation that reactant fluids are split into many fluid segments is often used to reduce mixing time. We have introduced two dimensionless numbers that represent effects of geometric design factors of fluid segments on reactor performance in reactors using this mixing operation: the ratio of reaction rate to diffusion rate ϕ and the

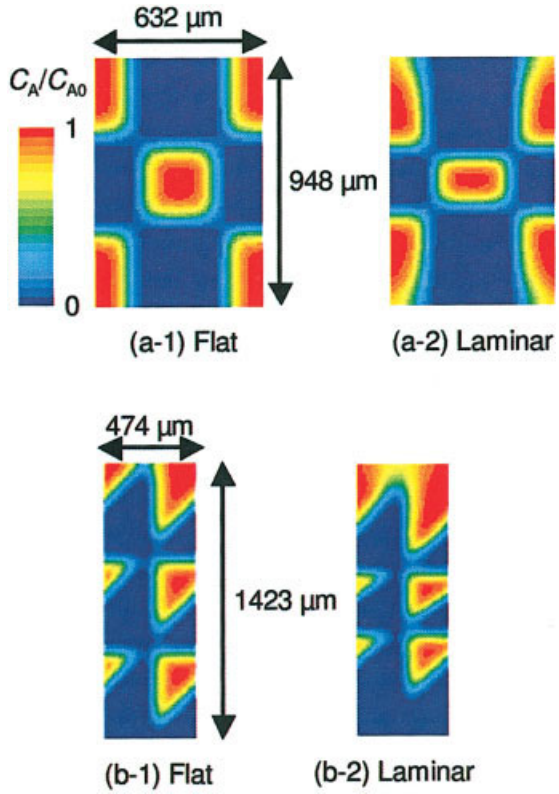

Figure 15. Effect of the laminar velocity distribution on the concentration profiles of A: (a) Rectangle-3 arrays; (b) Triangle-3 arrays.

$z = 0.001$ m. $\phi = 10^3$. [Color figure can be viewed in the online issue, which is available at www.interscience.wiley.com.]

aspect ratio of the mean diffusion length in the 2-D directions of the reactor cross section w. The geometric design factors of fluid segments applied in this article are an arrangement and a cross-sectional shape of fluid segments in the reactor inlet. We have also devised methods to determine the dimensionless numbers for a reactor of a set of the geometric design factors. These numbers can be used to predict reactor performance regardless of geometric design factors, and to determine geometric design factors of fluid segments giving desired reactor performance. To investigate the effectiveness of these numbers for these purposes, we have then compared product yields as a reactor performance measure between a pair of reactors having different arrangements and shapes of fluid segment, but the same dimensionless numbers using CFD simulations.

The results show that the order of ϕ allows us to determine whether reactions proceed under reaction controlled conditions even when the cross-sectional shape of fluid segments is changed. We can determine the largest size of fluid segments to achieve ideal mixing for reaction controlled conditions using the threshold value of ϕ. The threshold value of ϕ for reaction controlled conditions depends on the ratio of rate constants of multiple reactions. The second dimensionless number w can represent effects of arrangements and aspect ratios of cross-sectional shapes of fluid segments on the reactor performance. Product yields in reactors whose cross-sectional shape of fluid segments is a right-angled triangle have larger dependence on w than that of a rectangle. When we apply a right-angled triangle to the cross-sectional shape of fluid segments, the fluid segments need to be designed so that w is close to unity. From the concentration profile of reactants in the reactors, reactors whose cross-sectional shape of fluid segments is rectangle are favorable from the viewpoint that uniform mixing in the cross-sectional plane of reactor can be achieved especially when w takes large values. Moreover, the reactor performance for a reactor of a set of the dimensionless numbers with the laminar velocity distribution is comparable to or exceeds that by the estimate using the reactor of the identical dimensionless numbers with the flat velocity distribution. We also confirmed that Y_R of the reactors of other arrangements and cross-sectional shapes are independent of the velocity distribution when ϕ is the threshold value for reaction control conditions. Therefore, we can design fluid segments for microreactors with laminar flow velocity distribution using the threshold value of the dimensionless numbers for reaction controlled conditions derived from the approximation of the flat velocity distribution.

Besides mixing rate and product yield and selectivity, effects of the geometric design factors on the operability of microreactors are also essential issues. For example, the isothermal

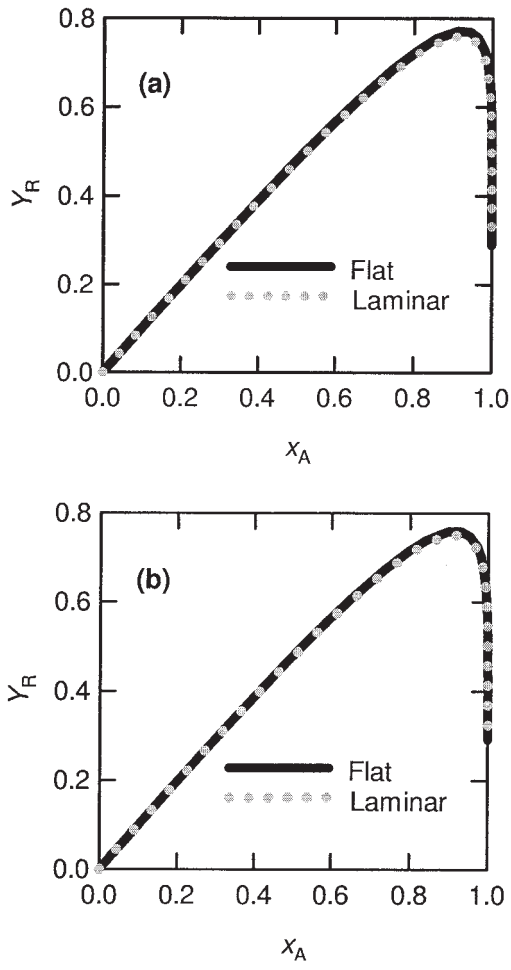

Figure 16. Effect of the laminar velocity distribution on the product yield: (a) Rectangle-3 arrays; (b) Triangle-1 array.

$\phi = 10^1$.

condition has been assumed in this study. The facility of the isothermal condition depends on the geometric design factors. For the design of fluid segments, the relation between the fabrication cost and the geometric design factors is also needed. Thus, this mixing operation would be designed from trade-off between product values, fabrication and operation costs.

Acknowledgments

We have conducted this research within the Project of Micro-Chemical Technology for Production, Analysis and Measurement Systems financially supported by the New Energy and industrial Development Organization (NEDO). We would also appreciate the Micro Chemical Plant Technology Union (MCPT) for their support.

Literature Cited

1. Jensen KF. Microreaction engineering-is small better? *Chem Eng Sci*. 2001;56:293-303.
2. Hessel V, Hardt S, Löwe H. *Chemical micro process engineering*. Weinheim, Germany: WILEY-VCH; 2004.
3. Ajmera SK, Losey MW, Jensen KF, Schmidt MA. Microfabricated packed-bed reactor for phosgene synthesis. *AIChE J*. 2001;47:1639-1647.
4. Chambers RD, Spink RCH. Microreactor for elemental fluorine. *Chem Commun*. 1999:883-884.
5. Yoshida J, Nagaki A, Iwasaki T, Suga S. Enhancement of chemical selectivity by microreactors. *Chem Eng Technol*. 2005;28:259-266.
6. Ehrfeld W, Golbig K, Hessel V, Löwe H, Richter T. Characterization of mixing in micromixers by a test reaction: single mixing units and mixer arrays. *Ind Eng Chem Res*. 1999;38:1075-1082.
7. Ehlers St, Elgeti K, Menzel T, Wieβmeier G. Mixing in the offstream of a microchannel system. *Chem Eng Proc*. 2000;39:291-298.
8. Löb P, Drese KS, Hessel V, Hardt S, Hofmann C, Löwe H, Schenk R. Schönfeld F, Werner B. Steering of liquid mixing speed in interdigital micro mixers-from very fast to deliberately slow mixing. *Chem Eng Technol*. 2004;27:340-345.
9. Kirner T, Albert J, Günther M, Mayer G, Reinhäckel K, Köhler JM. Static micromixers for modular chip reactor arrangements in two-step reactions and photochemical activated processes. *Chem Eng J*. 2004; 101:65-74.
10. Mae K, Maki T, Hasegawa I, Eto U, Mizutani Y, Honda N. Development of a new micromixer based on split/recombination for mass production and its application to soap free emulsifier. *Chem Eng J*. 2004;101:31-38.
11. Nagasawa H, Aoki N, Mae K. Design of a new micromixer for instant mixing based on collision of micro segment. *Chem Eng Technol*. 2005;28:324-330.
12. Stroock AD, Dertinger SKW, Ajdari A, Mezi I, Stone HA, Whitesides GM. Chaotic mixer for microchannels. *Science*. 2002;295:647-651.
13. Hong CC, Choi JW, Ahn CH. A novel in-plane passive microfluidic mixer with modified Tesla structures. *Lab Chip*. 2004;4:109-113.
14. Beebe DJ, Adrian RJ, Olsen MG., Stremler MA, Aref H, Jo B. Passive mixing in microchannels: fabrication and flow experiments. *Mec Ind*. 2001;2:343-348
15. Moctar A, Aubry ON, Batton J. Electro-hydrodynamic micro-fluidic mixer. *Lab Chip*. 2003;3:273-280.
16. Lu LH, Ryu KS, Liu C. A magnetic microstirrer and array for microfluidic mixing. *J Microelectromech Syst*. 2002;11:462-469.
17. Rife JC, Bell MI, Horwitz JS, Kabler MN, Auyeung RCY, Kim WJ. Miniature valveless ultrasonic pumps and mixers. *Sens Actuators B*. 2000;86:135-140
18. Ehlers St., Elgeti K, Menzel T, Wieβmeier G. Mixing in the offstream of a microchannel system. *Chem Eng Process*. 2000;39:291-298.
19. Hardt S, Schömnfeld F. Laminar mixing in different interdigital micromixers: II. numerical simulations. *AIChE J*. 2003;49:578-584.
20. Aoki N, Hasebe S, Mae K. Mixing in microreactors: effectiveness of lamination segments as a form of feed on product distribution for multiple reactions. *Chem Eng J*. 2004;101:323-331.
21. He S, Gotts JA. Calculation of friction coefficients for noncircular channels. *J Fluid Eng*. 2004;126:1033-1038.
22. Hitt DL, Macken N. A simplified model for determining interfacial position in convergent microchannel flows. *J Fluid Eng*. 2004;126: 758-767.
23. Aoki N, Hasebe S, Mae K. Design of feed segments: influences of sizes and shapes on product composition of multiple reactions. *2004 AIChE Annual Meeting* [CD-ROM]. Madison, WI: Omnipress; 2004: Paper 534b.
24. Paul EL, Atiemo-Obeng VA, Kresta SM. *Handbook of Industrial Mixing: Science and Practice*. Hoboken, NJ: John Wiley & Sons; 2004:33.
25. Street RL, Watters GZ, Vennard JK. *Elementary Fluid Mechanics.* 7th ed. New York, NY: John Wiley & Sons; 1996:50, 697.
26. Levenspiel O. *Chemical Reaction Engineering.* 3rd ed. New York, NY: John Wiley & Sons; 1998:190, 314-315.
27. *Fluent 6.2 User's Guide*. Lebanon, NH: Fluent inc.; 2005:Chapter 26.
28. Dombrowski N, Foumeny EA, Ookawara S, Riza A. The influence of Reynolds number on the entry length and pressure drop for laminar pipe flow. *Can J Chem Eng*. 1993;71:472-476.

Manuscript received May 10, 2005, and revision received Oct. 10, 2005.